CHEMISTRY
A EUROPEAN JOURNAL

FULL PAPER

DOI: 10.1002/chem.201301001

α-L-Fucosidase Inhibition by Pyrrolidine–Ferrocene Hybrids: Rationalization of Ligand-Binding Properties by Structural Studies

Audrey Hottin,[a] Daniel W. Wright,[b] Agata Steenackers,[c] Philippe Delannoy,[c] Faustine Dubar,[d, e] Christophe Biot,[c] Gideon J. Davies,[b] and Jean-Bernard Behr*[a]

Abstract: Enhanced metabolism of fucose through fucosidase overexpression is a signature of some cancer types, thus suggesting that fucosidase-targetted ligands could play the role of drug-delivery vectors. Herein, we describe the synthesis of a new series of pyrrolidine–ferrocene conjugates, consisting of a L-*fuco*-configured dihydroxypyrrolidine as the fucosidase ligand armed with a cytotoxic ferrocenylamine moeity. Three-dimensional structures of several of these fucosidase inhibitors reveal transition-state-mimicking ^3E conformations. Elaboration with the ferrocenyl moiety results in sub-micromolar inhibitors of both bovine and bacterial fucosidases, with the 3D structure of the latter revealing electron density indicative of highly mobile alkylferrocene compounds. The best compounds show a strong antiproliferative effect, with up to 100% inhibition of the proliferation of MDA-MB-231 cancer cells at 50 μM.

Keywords: antitumor agents · glycosidases · hydrolases · inhibition · protein structures

Introduction

The glycosylation of proteins located at the cell surface drives many biological events, such as cell–cell interactions, cell migration, bacterial adhesion, and viral invasion.[1] It has also been shown that perturbations of host glycans contributes to tumour invasion and metastasis.[2] An aberrant glycosylation pattern is associated with differential expression of the glycosidase and glycosyltransferase enzymes required for the biosynthesis of oligosaccharides. Among these, α-L-fucosidases (AFU) and fucosyltransferases (FucT) have received much attention due to the central role of fucosylated conjugates. Indeed, many antigenic oligosaccharides are functionalized by a terminal α-L-fucose moiety, thus suggesting that this 6-deoxyhexose acts as a physiopathological effector.[3] The biosynthesis and degradation of fucosides in vivo is performed by FucT and AFU, respectively, but the regulatory mechanisms for fucosylation are not fully understood. Nevertheless, elevated levels of both fucosyltransferases and fucosidases have been detected in various cancer tissues and the action of FucT and AFU during metastatic events is supported by several lines of evidence.[4] As a consequence of this overexpression, fucosidase is a potential receptor for selective targeting of cancer tissues. Ligands that display high affinity for fucosidases (or fucosyltransferases) should have utility as drug-delivery vectors for the detection or control of malignancy.[5] Herein, we focus on five-membered iminocyclitols as potent fucosidase ligands modified with a cytotoxic ferrocenylamine moiety.

Iminosugars are natural or synthetic sugar mimics in which the ring oxygen atom has been replaced by a nitrogen atom. At physiological pH value, the positively charged ammonium centre of imino and aza sugars (i.e., those in which a ring carbon atom has been replaced by a nitrogen atom) contributes to mimicry of the oxocarbenium ion-like transition state of the enzyme-catalyzed reaction and, facilitated by charge–charge interactions, gives rise to strong affinities (recently reviewed by Gloster and Davies[6a]). Indeed, whereas the dissociation constant K_M of a glycosidase–glycoside Michaelis complex ranges from 10 to 1000 μM, iminosugars show 3–6 orders of magnitude more potent affinities with K_i values in the micro- to nanomolar range.[6] Hence, iminosugars disrupt the normal processing of glycosidases (and to a lesser extent some glycosyltransferases); a proper-

[a] A. Hottin, Dr. J.-B. Behr
Université de Reims Champagne-Ardenne
Institut de Chimie Moléculaire de Reims, CNRS UMR 7312
UFR des Sciences Exactes et Naturelles
51687 Reims Cedex 2 (France)
Fax: (+33) 326913166
E-mail: jb.behr@univ-reims.fr

[b] D. W. Wright, Prof. G. J. Davies
Structural Biology Laboratory
Department of Chemistry
University of York, York YO10 5DD (UK)

[c] A. Steenackers, Prof. P. Delannoy, Prof. C. Biot
Université Lille Nord de France, Université Lille 1
Unité de Glycobiologie Structurale et Fonctionnelle
CNRS UMR 8576, IFR 147
59650 Villeneuve d'Ascq Cedex (France)

[d] Dr. F. Dubar
Université Lille Nord de France, Université Lille 1
Unité de Catalyse et Chimie du Solide, CNRS UMR 8181
59652 Villeneuve d'Ascq Cedex (France)

[e] Dr. F. Dubar
Present address: School of Chemistry
University of Glasgow, Glasgow, G12 8QQ (UK)

Supporting information for this article is available on the WWW under http://dx.doi.org/10.1002/chem.201301001.

ty that has been exploited for the development of new therapeutic agents.[7]

A number of fucosidase-inhibiting imino and aza sugars have been studied (Figure 1). Piperidines, exemplified by **1** and **2**, feature a specific fucopyranose-like stereochemical

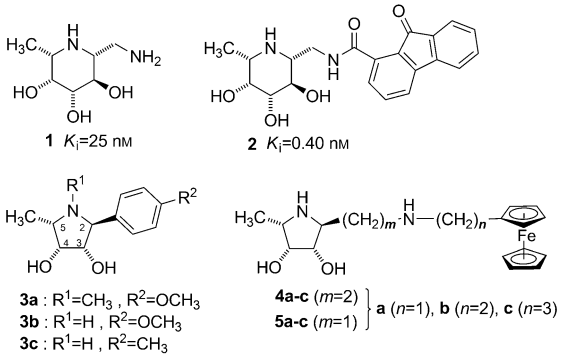

Figure 1. Structures of fucosidase inhibitors.

configuration and have been shown to be tightly binding inhibitors of fucosidase from various origins.[8] Intriguingly, five-membered iminocyclitols, such as **3** and **4**, show comparable performances, although they lack one hydroxy function in their structures.[9] Furthermore, the presence of aryl substituents in the pseudoanomeric position of either the piperidine or pyrrolidine framework improves the inhibition potencies, likely through hydrophobic effects in the aglycon binding pocket.[10] In contrast with the piperidine analogues,[11] so far little is known about the structural bases for AFU inhibition by five-membered iminocyclitols. Such information would aid the design of new potent ligands as therapeutic candidates.

We have previously reported ferrocene–iminocyclitol hybrids **4a–c** as the models of such drug-carrier conjugates.[12] In anticancer therapy, ferrocene (Fc) derivatives have been shown to generate a strong cytotoxic effect, which was related to the production of reactive oxygen species (ROS) through ferrocene-initiated Fenton reactions.[13] Structurally, compounds **4a–c** result from the combination of the cytotoxic ferrocenylamine moiety as the drug and an L-*fuco*-configured dihydroxypyrrolidine as the carrier. The resulting hybrids harness both the AFU binding properties and the cytotoxicity of each moiety alone. Among these compounds, **4c** was the most active of the series displaying $IC_{50}=1.2$ μM toward fucosidase and 77% growth inhibition of MDA-MB-231 breast-cancer cells at 50 μM. In continuation of our previous work, structure–activity relationship studies were extended to new analogues to uncover the mode of binding of these innovative organometallic inhibitors.

Herein, we describe the crystal structures of some five-membered iminocyclitols complexed with GH29 α-L-fucosidase from *Bacteroides thetaiotaomicron* (BtFuc2970) together with the synthesis and biological evaluation of ferrocenyl–pyrrolidines **5a–c**, **14**, and their purely organic phenyl analogues **12a**,**c** as both enzyme inhibitors and anticancer agents. The crystal structures of some five-membered iminocyclitols complexed with BtFuc2970 reveal a ^3E conformation for inhibitor binding, thus mimicking the postulated $^3H_4$ conformation of the catalytic transition state and, where present, clearly show the ferrocenyl moiety pointing toward the solvent molecules. The new compounds show sub-micromolar inhibition of fucosidase and antiproliferative action with up to 100% inhibition of MDA-MB-231 cancer cells proliferation at 50 μM.

Results and Discussion

Synthesis of fucosidase inhibitors: The synthesis of the target ferrocenyl–pyrrolidines **5a–c** was envisioned by coupling the cytotoxic ferrocenylamine moiety with a formyl–pyrrolidine species through reductive amination (Figure 2).

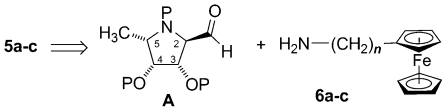

Figure 2. Synthetic access to new ferrocenyl iminosugars **5a–c**.

Whereas the required amines **6a–c** of general structure Fc-$(CH_2)_nNH_2$ ($n=1$, 2, and 3 for **6a–c**, respectively) may be obtained by following known synthetic procedures,[12] a multistep synthesis is required for the preparation of an enantiomerically pure formyl–pyrrolidine moiety such as **A**. A large panel of methods has been reported to access C2-functionalized iminocyclitols.[14] Among these methods, the addition of organometallic compounds to glycosylamines is particularly well suited and has been used with success for the synthesis of formyl–pyrrolidine derivatives related to other sugar series.[15] Thus, by using the ribose-derived *N*-benzylglycosylamine **7** as the starting material, 2-vinylpyrrolidine **8** was obtained in two steps after the stereoselective addition of vinylmagnesium bromide and subsequent treatment with methanesulfonyl chloride (Scheme 1). This method resulted in the selective formation of the targeted (2*S*)-2-vinylpyrrolidine **8**, which displays the required configuration for strong binding with AFU. Unfortunately, all our attempts to transform the double bond into a formyl group failed.

The direct ozonolysis of a tertiary amine such as **8** must be performed on the corresponding sulfate or hydrochloride salts to avoid oxidation at the nitrogen atom.[15a,c] In our case, the treatment of acid-sensitive **8** with either HCl or H_2SO_4 might lead to deprotection of the acetonide group. For this reason, ozonolysis was not attempted and we turned to a hydroxylation/periodate oxidation procedure. However, in contrast to the results obtained by Palmer and Jäger with an epimer of **8**,[16] bis-hydroxylation with either the OsO_4/*N*-methylmorpholine-*N*-oxide (NMO) system or with commercial AD-mix reagent failed. Coinciding with the disappearance of the starting material was the formation of overoxi-

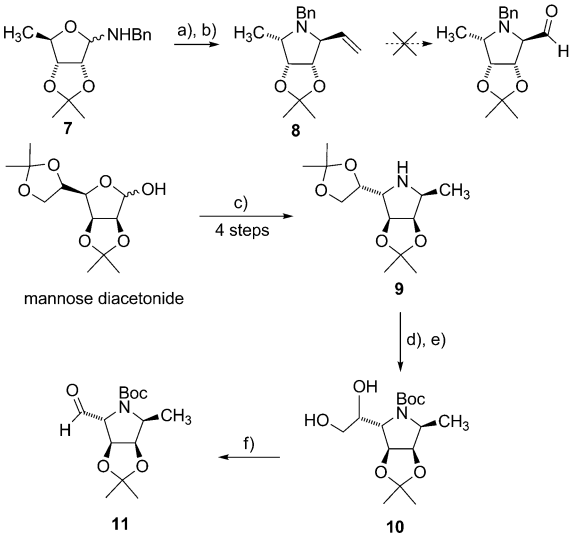

Scheme 1. Synthesis of formyl–pyrrolidine: a) vinylMgBr, THF, RT (83%); b) MsCl, pyr (77%); c) according to ref. [17]; d) Boc_2O, NEt_3, RT (97%); e) 60% aq. CH_3COOH (69%); f) $NaIO_4$, $EtOH/H_2O$ (100%). Boc = *tert*-butoxycarbonyl, Ms = methanesulfonyl, pyr = pyridine.

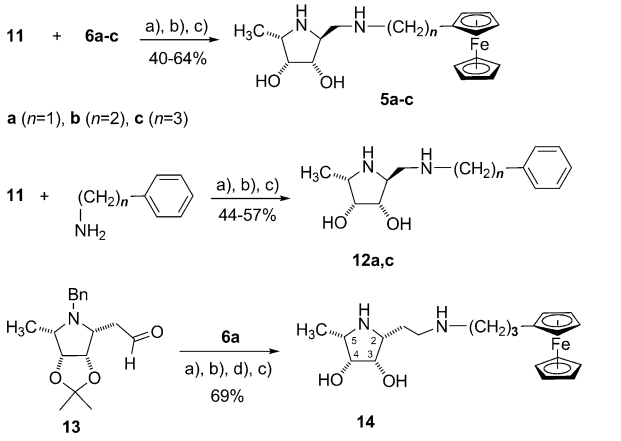

Scheme 2. Coupling by reductive amination. a) $MgSO_4$, CH_2Cl_2; b) $NaBH_4$, MeOH; c) 1 M HCl, MeOH then Amberlyst A-26 (OH^-); d) H_2, Pd–C.

dation and open-chain products, the latter probably resulted from an intramolecular Cope elimination. Thus, we turned to an alternative synthesis of the required formyl–pyrrolidine, which started with D-mannose diacetonide. A four-step sequence yielded methylpyrrolidine **9**,[17] the stereochemical configuration of which matched that required for potent inhibition of AFU. Using protected **9** as its *N*-Boc derivative, selective hydrolysis of the primary acetonide afforded the expected diol **10** in an acceptable yield (67%). Subsequent oxidative cleavage with sodium periodate gave the 2-formyl–pyrrolidine **11** (the enantiomer of which has previously been prepared using another strategy[18]). Carboxaldehyde **11** was used in the coupling procedure without further purification.

The attachment of a ferrocenylamine moiety to **11** was accomplished by using reductive amination (Scheme 2). To achieve this goal, each amine **6a–c** was treated with **11** in CH_2Cl_2 in the presence of $MgSO_4$ as a dehydrating agent to yield the corresponding imine. After filtration and concentration of the reaction mixture, the residue was dissolved in MeOH and sodium borohydride was added to allow reduction to the expected amine. Final deprotection of the acid-labile groups was performed in 1 M HCl. Ferrocenyl iminosugars **5a–c** were obtained in a pure form (40–64% overall yield from **11**) after neutralization with Amberlyst A-26 (OH^- form) and purification by chromatography on silica gel.

Several analogues were prepared in the same manner (Scheme 2). Compounds **12a**,**c**, which feature a phenyl group in place of ferrocene, were isolated after the coupling of carboxaldehyde **11** with benzylamine or commercial 3-phenylpropylamine. Furthermore, ferrocenyl iminosugar **14**, the C2 epimer of the known **4c**, featured a β-configured substituent at C2, that is, the opposite stereochemistry to natural α-L-fucosidase substrates and inhibitors **3–5**. The synthesis of **14** used carboxaldehyde **13**[12] as the starting material and was accomplished following similar reaction sequences.

Enzyme inhibition and antiproliferative activity: The fucosidase inhibition, both of the α-L-fucosidase from bovine kidney and, for selected compounds, the BtFuc2970 enzyme from *Bacteroides thetaiotaomicron* as well as the antiproliferative potential (against MDA-MB-231 breast-cancer cells) of new compounds **5a–c**, **12a**,**c**, and **14** were evaluated and compared to analogues **3a–c** and **4a–c** (Table 1). Compounds **5a–c** displayed K_i values toward bovine kidney AFU in the sub-micromolar range (K_i = 0.19–0.22 μM), thus the presence of the ferrocene functionality did not impede binding of the pyrrolidine unit to fucosidase (see below for comparison with the non-ferrocenyl analogues).

Ferrocenyliminocyclitols bind to bovine kidney α-L-fucosidase much more tightly than the substrate *para*-nitrophenyl-α-L-fucopyranoside (K_M = 640 μM). Compounds **5a–c** were slightly better inhibitors of AFU than the reported homologues **4a–c** (K_i = 0.29-0.39 μM). Moreover, in each series, increasing the length of the carbon chain that connects the pyrrolidine to the ferrocenyl unit (**a–c**) led to more potent affinities. This was also observable with the non-ferrocenyl analogues because **12c** (n = 3, K_i = 0.24 μM) binds more tightly to AFU than **12a** (n = 1, K_i = 0.57 μM). This result is in contrast with the data obtained from arylpyrrolidines **3a–c**, in which the presence of the aryl group in proximity to the fucose surrogate afforded better affinities (K_i = 10 nM). Interestingly, the ferrocenyl-containing derivative **5c** (K_i = 0.19 μM) was an even more potent inhibitor than the control compound **12c** (K_i = 0.24 μM), an analogue that features a less sterically demanding phenyl group. Results from Table 1 also show that only the 2*S* configuration in the pyrrolidine ring provides an adequate orientation of the C2 "aglycon" substituent to induce strong binding to AFU, that is, **14**

Table 1. Fucosidase inhibition and antiproliferative effect (breast-cancer cells) of aryl– and ferrocenyl–pyrrolidines.[a]

Inhibitor	Structure	Inhibition of bovine kidney AFU K_i [μM]	Inhibition of MDA-MB-231 cell growth (% control) $[I]=50$ μM	$[I]=25$ μM
3a	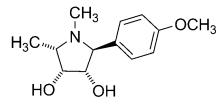	0.81[c]	nd	nd
3b	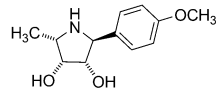	0.0095[c]	nd	ni
3c	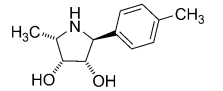	0.010[c]	nd	nd
4a	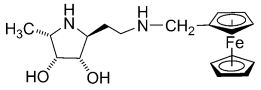	0.29	ni[b]	ni[b]
4b	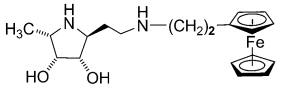	0.39	45 ± 19[b]	ni[b]
4c	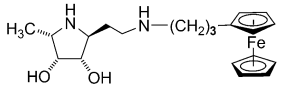	0.29	77 ± 30[b]	39 ± 16[b]
5a	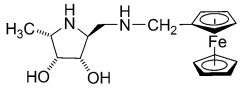	0.21	ni	ni
5b	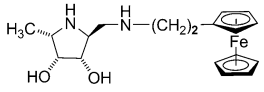	0.22	40 ± 17	15 ± 14
5c	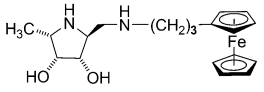	0.19	75 ± 6	42 ± 19
12a	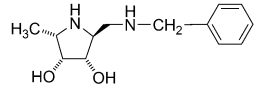	0.57	ni	nd
12c	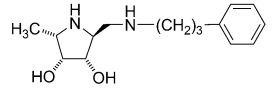	0.24	ni	nd
14	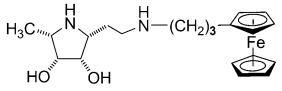	7.3	100 ± 1.5	32 ± 6

[a] ni = no inhibition, nd = not determined. [b] Taken from ref. [12]. [c] Taken from ref. [10c].

($K_i = 7.3$ μM) was 25-fold less active than its 2*S* counterpart **4c** toward fucosidase.

Prior to structural analysis, tight binding to the bacterial enzyme was confirmed. The inhibition of BtFuc2970 by **3a**,**b** and **4a**,**c** ($K_i = 5.4$, 3.5, 0.52, and 0.46 μM, respectively) was studied (see the Supporting Information). Unfortunately, insufficient compound was available to determine a K_i value for **3c**, which displayed potent inhibition toward bovine-kidney α-L-fucosidase, similar to the analogue **3b** (Table 1). Contrasting results were obtained with both fucosidase sources; that is, although ferrocenyl iminosugars **4a**,**c** had weaker affinities than the arylpyrrolidines **3a–c** for fucosidase from bovine kidney, they were significantly better ligands of BtFuc2970.

Next, the antiproliferative effect was analyzed by using the hormone-independent breast-cancer cell-line MDA-MB-231, which had previously shown to be sensitive to ferrocene conjugates.[19] Inhibition of cell growth was determined at two concentrations of the drug (25 and 50 μM) and was evaluated by comparison with an untreated control. The antiproliferative activity of ferrocenyliminocyclitols **5a–c** was similar to that previously observed for compounds **4a–c** depending on the length (*n*) of the side chain of the ferrocenylamine moiety (Table 1).[12] No antiproliferative activity was observed for **5a** at the highest concentration, whereas inhibition of 40 and 75% was observed with **5b** and **5c**, respectively. On the other hand, the number (*m*) of methylene groups between the iminosugar and the ferrocenylamine moieties does not significantly impact the antiproliferative effect of **5a–c** relative to **4a–c**. As expected, no antiproliferative activity was obtained with the phenyl-containing analogues **12a** and **12c** or with the arylpyrrolidine **3b** alone, thus confirming that only the ferrocenyl moiety is responsible for the antiproliferative action. Finally, results from Table 1 also show that the configuration in the pyrrolidine ring has no effect on the antiproliferative activity of the ferrocenyliminocyclitols, with **14** being as active as its 2*S* counterpart **4c**, thus showing there is no direct relationship between the tightness of fucosidase binding and the antiproliferative activities. Thus, conjugation of the cytotoxic ferrocenylamine moiety to the pyrrolidine unit did not decrease its antiproliferative action. This outcome was also evidenced by the similarity between the cell-growth curves in presence of a ferrocenylamine moiety alone and after conjugation to the pyrrolidine ring (see the Supporting Information).

Structural analysis of fucosidase inhibition: A number of 3D structures for fucosidases from the carbohydrate-active enzyme (CAZY) family GH29 have previously been determined including α-L-fucosidases from *Thermotoga maritima*,[20] *Bacteroides thetaiotaomicron*,[11b] and *Bifidobacterium longum*.[21] To date, no structural information is available for mammalian fucosidases and the *Bacteroides thetaiotaomicron* (BtFuc2970) enzyme can act as a reasonable surrogate with sequence identity with human GH29 fucosidases FUCA1 and FUCA2 of 27 and 28%, respectively.

Crystal structures of BtFuc2970 with **3a–c** and **4a**,**c** as ligands were obtained (details of the data collection and refinement are given in the Supporting Information) to elucidate the structural factors that determine the potency of the inhibition of fucosidase. The presence of inhibitors **3a–c** in their crystal structures was immediately apparent from difference maps, whereas the presence of **4a** and **4c** became apparent after a number of cycles of refinement (Figure 3). The *fuco*-configured ring systems of all the inhibitors adopt

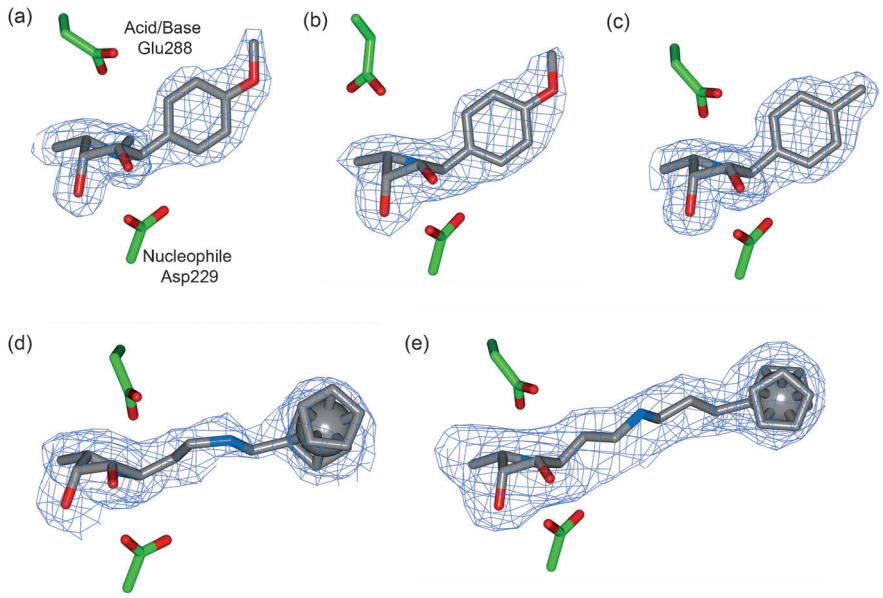

Figure 3. Inhibitors a) **3a**, b) **3b**, c) **3c**, d) **4a**, and e) **4c** that lie in the BtFuc2970 active site. Maps shown are F_o–F_c maps contoured at 5 σ (**3a**–**c**) or 3 σ (**4a**,**c**), in each case calculated by using phases prior to the incorporation of the ligand in refinement. The enzymatic acid/base and nucleophile are shown and labeled in (a).

^3E envelope conformations. The "aglycon" moieties of these inhibitors lay atop a hydrophobic ridge formed by residues tryptophan 88 (Trp88) and Trp232 and point toward the solvent molecules in contrast to the "aglycons" for six-membered inhibitors.[11b]

Compound **3a** has an *N*-methylated endocylic amine and displays only a slight difference in binding affinity relative to its parent compound **3b**, which lacks *N*-methylation (K_i = 5.4 vs. 3.5 μM), thus indicating that BtFuc2970 can easily accommodate the extra steric bulk. This finding can be observed in the crystal structures, with only minimal differences observed between the structures of **3a** and **3b**. The *N*-methyl group of **3a** disrupts a hydrogen-bonding interaction that exists between a water molecule and the catalytic nucleophile aspartic acid 229 (Asp229) in the complex with **3b** (see the Protein Data Bank (PDB), entry 4JFT). Additionally, arginine 262 (Arg262) is slightly displaced toward the catalytic acid/base in the complex with **3a** (see the PDB, entry 4JFS) and forms hydrogen bonds with this residue. *N*-Methylation seems much more detrimental for the binding with bovine-kidney protein because the K_i value increases from 10 nM to 3.5 μM for **3b** and alkylated **3a**, respectively.

The ferrocenyl "aglycon" moieties of **4a** and **4c** are highly disordered. The presence of the ferrocene group in the crystal structure was confirmed through the collection of diffraction data for BtFuc2970 with **4a** as a ligand at $\lambda = 1.2$ Å and a significant "anomalous" signal was observed (Figure 4). The ferrocenyl "aglycons" interact through Van der Waals' forces, which has been observed previously in ferrocenyl enzyme/inhibitor complexes.[22] The fact that the ferrocenyl moieties of **4a**,**c** point toward the solvent molecules rather than being buried in a hydrophobic pocket (as do the ferrocene complexes in ref. [22]) explains the high temperature-factors observed. The exocyclic amine that tethers the ferrocene and pyrrolidine groups is invariantly coordinated to a sulfate moiety likely abstracted from the crystallization liquor (Figure 4).

The small-molecule crystal structure of **3a** has already been determined.[10c] Interestingly, the conformations observed for **3a** in both the free-state and enzyme-bound crystal structures appear to be almost identical (0.18 Å root-mean square deviation; see the Supporting Information). Hence, binding of pyrrolidines, such as **3**, occurs without energy-demanding conformational distortion of the ligand to match the shape of the enzyme catalytic site, which could explain, at least in part, the strong affinities of our five-membered fucose mimics for fucosidases.

Conclusion

Five-membered iminosugars display potent affinities for fucosidases. This particular property could be exploited for the selective delivery of antitumor drugs toward fucosidase-rich malignant tissues. We prepared a series of iminosugar–

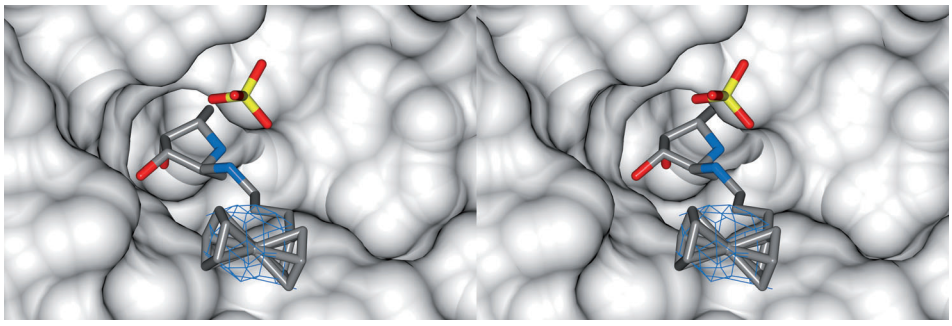

Figure 4. Surface representation, in divergent ("wall-eyed") stereo of the active site of BtFuc2970 with **4c**. The inhibitor atoms are displayed as cylinders (carbon atoms in gray, others colored by atom type). The map shown is an anomalous difference map (averaged over the unit cell) contoured at 5 σ. The protein atoms of BtFuc2970 from 4JFW are displayed as a white surface.

ferrocene hybrids, which retained both the fucosidase inhibition capability of the iminocyclitol moiety and the cytotoxicity of the ferrocenylamine species. Comparison with control analogues, which either lack the ferrocenyl functionality or bind much less tightly to the AFU, clearly showed the pyrrolidine unit to have no cytotoxic effect on its own, with all the antiproliferative activity being potentiated by the ferrocenyl moiety. Little is known about the structural basis for AFU inhibition by polyhydroxypyrrolidines. Crystal structures of a number of five-membered iminocyclitols bound to α-L-fucosidase BtFuc2970 were obtained to identify the factors that determine the potency of binding. These structures revealed that pyrrolidines adopt a ^3E envelope conformation in the active site, thus mimicking the proposed $^3H_4$ conformation for the catalytic transition state. It is this conformation that the inhibitor also adopts in its small-molecule crystal structure. Interestingly, the ferrocenyl moiety of the ferrocene-containing inhibitors points toward the solvent molecules, being available for the generation of ROS by being in contact with the biological environment in vivo.

In the near future, we intend to evaluate the ability of our compounds to cross cancer tissues selectively in vivo to lay the foundations of such a therapeutic approach.

Experimental Section

General: All the reactions were performed under argon. The reagents and solvents were commercially available in high purity and used as received. Silica gel F254 (0.2 mm) was used for the TLC plates and detection was carried out by spraying with an alcoholic solution of phosphomolybdic acid, *para*-anisaldehyde, or an aqueous solution of $KMnO_4$ (2%)/Na_2CO_3 (4%), followed by heating. Flash column chromatography was performed over silica gel M 9385 (40–63 μm) Kieselgel 60. NMR spectra were recorded on Bruker AC250 (250 and 62.5 MHz for ^1H and ^{13}C nuclei, respectively) or 600 (600 and 150 MHz for ^1H and ^{13}C nuclei, respectively) spectrometers. Chemical shifts are expressed in parts per million (ppm) and were calibrated to the residual solvent peak. Coupling constants are in Hz and the splitting pattern abbreviations are br = broad, s = singlet, d = doublet, t = triplet, q = quartet, qt = quintuplet, and m = multiplet. IR spectra were recorded with an IR plus MIDAC spectrophotometer and are expressed in cm^{-1}. Optical rotations were determined at 20°C with a Perkin–Elmer Model 241 polarimeter in the specified solvents. High-resolution mass spectrometry (HRMS) was performed on Q-TOF Micro micromass positive ESI (CV = 30 V).

Synthesis of vinylpyrrolidine 8: Vinylmagnesium bromide (30.6 mL of a commercial 1 M solution, 30.6 mmol, 4 equiv) was added dropwise to a stirred solution of glycosylamine **7** (1.990 g, 7.66 mmol) in THF (20 mL) at 0°C. The resulting mixture was left at room temperature for 7 h. Saturated NH_4Cl was added to the reaction mixture, and the solution was extracted with Et_2O (3 × 20 mL). The combined organic layers were dried ($MgSO_4$) and evaporated. Purification by flash column chromatography (EtOAc/petroleum ether 4:6) yielded the intermediate aminoalcohol (R_f = 0.43, 1.162 g, 52%) as a yellow oil.

MsCl (640 μL, 8.175 mmol, 2.45 equiv) was added dropwise to a solution of pure aminoalcohol (1.082 g, 3.715 mmol) in pyridine (4.7 mL) and THF (4.7 mL) at 0°C. The mixture was stirred for 2 h at 0°C and for an additional 2 h at room temperature. Saturated solutions of NH_4Cl and Et_2O were successively added at 0°C, and the resulting organic phase was separated. The aqueous layer was extracted with Et_2O and the combined organic layers were dried over $MgSO_4$ and concentrated. The residue was purified by chromatography on silica gel (Et_2O/petroleum ether 1:9) to yield pure allylpyrrolidine **8** (783 mg, 77%) as a yellow oil.

Compound 8 (77%, yellow oil): R_f = 0.87 (Et_2O/petroleum ether 3:7); $[\alpha]_D^{20}$ = +7.1 (c = 0.54 in $CHCl_3$); IR (film): $\tilde{\nu}_{max}$ = 878, 1000, 1063, 1123, 1160, 1209, 1378, 1454, 2806, 2933, 2984 cm^{-1}; ^1H NMR (250 MHz, $CDCl_3$): δ = 1.13 (d, $^3J_{HH}$ = 6.3 Hz, 3H; 6-H), 1.34 (s, 3H; *i*Pr), 1.57 (s, 3H; *i*Pr), 2.90–3.08 (m, 1H; 5-H), 3.38–3.57 (m, 2H; 2-H and CH_2-Ph), 3.82 (d, $^2J_{HH}$ = 14.1 Hz, 1H; CH_2-Ph), 4.40–4.43 (m, 1H; 3-H), 4.61 (t, $^3J_{HH}$ = 5.7 Hz, 1H; 4-H), 5.12 (dd, J_{HH} = 50.0, 13.7 Hz, 2H; 2′-H), 5.62–5.82 (m, 1H; 1′-H), 7.14–7.40 ppm (m, 5H; Ar); ^{13}C NMR (62.5 MHz, $CDCl_3$): δ = 12.45 (6-C), 25.59 and 26.43 (*i*Pr), 50.45 (CH_2-Ph), 58.59 (5-C), 68.85 (2-C), 81.74 (4-C), 83.79 (3-C), 119.39 (2′-C), 126.48, 128.04 and 128.24 (Ar), 133.60 ppm (1′-C); HRMS (ESI): m/z calcd for $C_{17}H_{23}NO_2$: 274.1807 $[M+H^+]$; found: 274.1810.

Synthesis of aldehyde 11: Boc_2O (459 mg, 2 mmol, 1.1 equiv) was added in small portions to methylpyrrolidine **9**[17] (344 mg, 1.338 mmol) in CH_2Cl_2 (5 mL) and Et_3N (470 μL, 4.014 mmol, 3 equiv) at 0°C. The reaction mixture was allowed to warm slowly to room temperature and was stirred for additional 24 h. Distilled water (20 mL) was added to the mixture, and the separated aqueous layer was extracted with dichloromethane (3 × 20 mL). The combined organic layers were dried ($MgSO_4$), filtered, and evaporated under reduced pressure. The crude residue was purified by column chromatography on silica gel (EtOAc/petroleum ether 1:9) to afford the *N*-Boc derivative (462 mg, 97%,) as a white solid.

This protected pyrrolidine (153 mg, 0.428 mmol) in 60% aq. CH_3COOH (5 mL) was stirred 15 h at room temperature. The volatiles were evaporated under reduced pressure and after purification by column chromatography on silica gel (petroleum ether/EtOAc 4:6) the expected diol **10** (94 mg, 69%) was obtained as a yellow oil.

Diol 10 (69%, yellow oil): $[\alpha]_D^{20}$ = +44.9 (c 0.79, $CDCl_3$); ^1H NMR (250 MHz, $CHCl_3$): δ = 1.32 (s, 6H; *i*Pr, CH_3), 1.45 (s, 12H; *i*Pr, Boc), 3.35–3.59 (m, 2H; 2′-H), 3.81–3.98 (m, 2H; 5-H and 1′-H), 4.15–4.30 (m, 1H; 2-H), 4.51–4.67 ppm (m, 2H; 3-H and 4-H); ^{13}C NMR (63 MHz $CDCl_3$): δ = 16.11 (CH_3), 25.18, 26.24, 28.46 (2 × *i*Pr and Boc), 58.27 (5-C), 63.46 (2′-C), 63.82 (2-C), 73.60 (1′-C), 81.14, 81.55 ppm (3-C and 4-C); HRMS (ESI): m/z calcd for $C_{15}H_{27}NO_6$: 340.1736 $[M+Na]^+$; found: 340.1744.

$NaIO_4$ (170 mg, 0.797 mmol, 2.7 equiv) was added to diol **10** (94 mg, 0.305 mmol) in EtOH/water (6 mL, 2:1). The solution was stirred at room temperature for 1 h, then water (10 mL) and dichloromethane were added. After separation of the layers, the aqueous phase was washed with dichloromethane (3 × 10 mL). The combined organic layers were dried ($MgSO_4$), filtered, and evaporated to afford the crude aldehyde **11** (85 mg, 100%, yellow oil), which was used in the next step without further purification.

General procedure for the synthesis of hybrids 5, 12, and 14: $MgSO_4$ (119 mg, 1.00 mmol, 10 equiv) and ferrocenylamine **5** (1.2 equiv) were successively added to aldehyde **11** (35 mg, 0.100 mmol) in dichloromethane (1.5 mL). The solution was stirred at room temperature for 5 h. The solution was filtered and concentrated. $NaBH_4$ (5 mg, 0.130 mmol, 1.3 equiv) was added to the resulting material dissolved in MeOH (2 mL) at 0°C. This solution was stirred and left to warm to room temperature overnight. A saturated solution of NH_4Cl and EtOAc were successively added at 0°C, and the resulting organic layer was separated. The aqueous layer was extracted with EtOAc, and the combined organic layers were dried over $MgSO_4$ and concentrated. The residue was purified by chromatography on silica gel (EtOAc) to yield pure the ferrocenyl iminosugar.

The solution of ferrocenyl iminosugar (0.042 mmol) in MeOH (1 mL) was treated with 3 M HCl (1 mL). The mixture was stirred at room temperature overnight. After completion of the reaction the solution was neutralized with Amberlyst A-26 (OH^-) and evaporated. Purification by column chromatography on silica gel (dichloromethane/MeOH 8:2 → $CHCl_3$/MeOH/1 M NH_4OH 6:4:1) yielded ferrocenyl iminosugar **5** as a yellow film.

Compound 5a (64% from **10**): $[\alpha]_D^{20}$ = −25.0 (c = 0.76 in MeOH); ^1H NMR (600 MHz, MeOD): δ = 1.21 (d, $^3J_{HH}$ = 6.7 Hz, 3H; CH_3), 2.71 (dd, $^3J_{HH}$ = 12.3, 8.6 Hz, 1H; 1′-H), 2.86 (dd, $^3J_{HH}$ = 12.3, 4.7 Hz, 1H; 1′-H), 3.22 (qd, $^3J_{HH}$ = 6.7, 2.9 Hz, 1H; 2-H), 3.27 (td, $^3J_{HH}$ = 8.2, 4.7 Hz, 1H; 5-H), 3.64 (s, 2H; 2′-H), 3.81–3.84 (m, 1H; 4-H), 3.86 ppm (dd, $^3J_{HH}$ = 7.7,

4.1 Hz, 1H; 3-H); ^{13}C NMR (63 MHz, MeOD): δ=12.82 (CH_3), 49.24, 49.62 (1′,2′-C), 57.82, 60.93 (2,5-C), 69.73, 70.57 (Fc), 74.00 (4-C), 76.7 (3-C), 81.63 ppm (Cq-Fc) HRMS (ESI): *m/z* calcd for $C_{17}H_{24}FeN_2O_2$: 345.1265 $[M+H]^+$; found: 345.1263.

Compound 5b (40% from **10**): $[\alpha]_D^{20}=-11.5$ (c=0.4 in MeOH); ^{1}H NMR (600 MHz, D_2O): δ=1.14 (d, $^3J_{HH}$=6.7 Hz, 3H; CH_3), 2.52 (t, $^3J_{HH}$=7.6 Hz, 2H; NCH_2CH_2Fc), 2.68 (dd, $^3J_{HH}$=12.3, 8.6 Hz, 1H; 1′-H), 2.73–2.79 (m, 2H; NCH_2 CH_2Fc), 2.81 (dd, $^3J_{HH}$=12.3, 4.4 Hz, 1H; 1′-H), 3.17 (qd, $^3J_{HH}$=6.4, 2.7 Hz, 1H; 5-H), 3.20–3.22 (m, 1H; 2-H), 3.72–3.78 (m, 1H; 4-H), 3.81 ppm (dd, $^3J_{HH}$=7.8, 4.0 Hz, 1H; 3-H); ^{13}C NMR (63 MHz, D_2O): δ=13.88 (CH_3), 30.21 (NCH_2CH_2Fc), 51.58 (NCH_2CH_2Fc), 52.80 (1′-C), 56.91 (5-C), 61.69 (2-C), 68.50, 69.26, 69.56 (3×Fc), 74.91 (4-C), 77.91 (3-C), 86.89 ppm (Cq-Fc); HRMS (ESI): *m/z* calcd for $C_{18}H_{26}FeN_2O_2$: 359.1422 $[M+H]^+$; found: 359.1432.

Compound 5c (59% from **10**): $[\alpha]_D^{20}=-20.9$ (c=0.38 in MeOH); ^{1}H NMR (600 MHz, MeOD): δ=1.29 (d, $^3J_{HH}$=6.7 Hz, 3H; CH_3), 1.77–1.88 (m, 2H; $CH_2CH_2CH_2Fc$), 2.39–2.49 (m, 2H; $CH_2CH_2CH_2Fc$), 2.86 (qt, $^3J_{HH}$=11.9, 7.4 Hz, 2H; $CH_2CH_2CH_2Fc$), 2.95 (dd, $^3J_{HH}$=12.9, 9.1 Hz, 1H; 1′-H), 3.09 (dd, $^3J_{HH}$=12.9, 4.2 Hz, 1H; 1′-H), 3.43 (m, 2H; 2,5-H), 3.89–3.93 (m, 1H; 3-H), 3.99 (dd, $^3J_{HH}$=8.0, 3.8 Hz, 1H; 4-H), 4.05–4.15 ppm (m, 9H; Fc); ^{13}C NMR (151 MHz, MeOD): δ=13.04 (CH_3), 27.96 ($NCH_2CH_2CH_2Fc$), 30.55 ($NCH_2CH_2CH_2Fc$), 49.79 ($NCH_2CH_2CH_2Fc$), 50.84 (1′-C), 57.68 (5-C), 60.99 (2-C), 68.34, 69.06, 69.52 (3×Fc), 74.25 (3-C), 76.93 (4-C), 89.10 ppm (Cq-Fc); HRMS (ESI): *m/z* calcd for $C_{19}H_{28}FeN_2O_2$: 373.1578 $[M+H]^+$; found: 373.1571.

Compound 12a (57% from **10**): $[\alpha]_D^{20}=-0.05$ (c=0.2 in MeOH); ^{1}H NMR (600 MHz, D_2O): δ=1.12 (d, $^3J_{HH}$=6.7 Hz, 3H; CH_3), 2.67 (dd, $^3J_{HH}$=12.3, 8.9 Hz, 1H; 1′-H), 2.81 (dd, $^3J_{HH}$=12.3, 4.4 Hz, 1H; 1′-H), 3.18 (qd, $^3J_{HH}$=6.6, 2.8 Hz, 1H; 5-H), 3.24 (td, $^3J_{HH}$=8.3, 4.4 Hz, 1H; 2-H), 3.81 (s, 2H; NCH_2Ph), 3.89–3.94 (m, 2H; 3 and 4-H), 7.30–7.50 ppm (m, 5H; Ar); ^{13}C NMR (63 MHz, D_2O): δ=13.49 (CH_3), 51.83 (1′-C), 52.89 (NCH_2Ph), 55.04 (5-C), 60.01 (2-C), 74.26, 76.93 (3 and 4-C), 128.01, 129.15 ppm (3×Ar); HRMS (ESI): *m/z* calcd for $C_{13}H_{20}N_2O_2$: 237.1603 $[M+H]^+$; found: 237.1602.

Compound 12c (44% from **10**): $[\alpha]_D^{20}=-28.0$ (c=0.5 in MeOH); ^{1}H NMR (500 MHz, D_2O): δ=1.14 (d, $^3J_{HH}$=6.7 Hz, 3H; CH_3), 1.88–1.97 (m, 2H; $NCH_2CH_2CH_2Fc$), 2.71 (t, $^3J_{HH}$=7.6 Hz, 2H; NCH_2CH_2 CH_2Fc), 2.78–2.87 (m, 3H; N $CH_2CH_2CH_2Fc$ and 1′-H), 2.97 (dd, $^3J_{HH}$=12.6, 4.3 Hz, 1H; 1′-H), 3.20 (qd, $^3J_{HH}$=6.7, 2.9 Hz, 1H; 5-H), 3.28 (td, $^3J_{HH}$=8.6, 4.3 Hz, 1H; 2-H), 3.90–3.94 (m, 1H; 4-H), 3.97 (dd, $^3J_{HH}$=8.1, 4.1 Hz, 1H; 3-H), 7.25–7.34 (m, 3H; Ar), 7.37–7.43 ppm (m, 2H; Ar); ^{13}C NMR (62 MHz, D_2O): δ=13.27 (CH_3), 28.65 ($NCH_2CH_2CH_2Fc$), 32.58 ($NCH_2CH_2CH_2Fc$), 48.25 ($NCH_2CH_2CH_2Fc$), 51.51 (1′-C), 55.38 (5-C), 58.70 (2-C), 74.05 (4-C), 76.69 (3-C), 126.73, 128.91, 129.15 ppm (3× Ar); HRMS (ESI): *m/z* calcd for $C_{15}H_{25}N_2O_2$: 265.1916 ($[M+H]^+$; found: 265.1911.

Compound 14 (69% from **13**): $[\alpha]_D^{20}=+0.4$ (c=1 in MeOH); ^{1}H NMR (600 MHz, MeOH): δ=1.38 (d, $^3J_{HH}$=6.8 Hz, 3H; CH_3), 1.86–1.99 (m, 3H; $NCH_2CH_2CH_2Fc$), 2.10 (dq, $^3J_{HH}$=8.6, 6.7 Hz, 1H; 1′a-H), 2.28 (ddd, $^3J_{HH}$=15.2, 11.3, 6.7 Hz, 1H; 1′b-H), 2.43–2.51 (m, 2H; $NCH_2CH_2CH_2Fc$), 2.98–3.06 (m, 2H; $NCH_2CH_2CH_2Fc$), 3.10–3.23 (m, 2H; 2′-H), 3.54–3.61 (m, 1H; 5-H), 3.62–3.68 (m, 1H; 2-H), 4.20 (t, $^3J_{HH}$=4.8 Hz, 41H; -H), 4.36 ppm (dd, $^3J_{HH}$=6.2, 4.8 Hz, 1H; 3-H); ^{13}C NMR (151 MHz, MeOD): δ=12.78 (CH_3), 25.54 (1′-C), 27.59 ($NCH_2CH_2CH_2Fc$), 28.92 ($NCH_2CH_2CH_2Fc$), 45.93 (2′-C), 57.85 (5-C), 59.05 (2-C), 68.46, 69.05, 69.57 (3xFc), 71.93 (3-C), 72.57 (4-C), 88.32 ppm (Cq-Fc); HRMS (ESI): calcd for $C_{20}H_{30}FeN_2O_2$: 387.1735 $[M+H]^+$; found: 387.1722.

Fucosidase inhibition assays

Bovine kidney fucosidase: Compounds were assayed according to a reported procedure.[12] Enzyme activity was determined at 35°C (acetate buffer, pH 5.6) after incubation of 2 mM *para*-nitrophenyl fucoside for 15 min and quenching the reaction by addition of 0.8 M sodium carbonate. The *para*-nitrophenolate formed was quantified at λ=410 nm. The inhibitors were preincubated at 35°C for 5 min with the fucosidase before the addition of the substrate. At least five concentrations of each compound were tested, and the IC_{50} values were determined by using Dixon plots. The inhibition constants K_i were calculated according to the Cheng–Prusoff equation. All the assays were done in duplicate (less than 10% variability in each case).

BtFuc2970: Substrate 2-chloro-4-nitrophenyl-α-L-fucopyranoside (CNP-fucoside) was purchased from Carbosynth Ltd. The experiments were run over a time course of 5 min during which absorbance at λ=405 nm was detected. For each data point, a solution of 50 mM HEPES buffer (pH 700 mM NaCl 250 nM *Bt*Fuc2970 was equilibrated thermally (37°C) in the presence of a varying concentration (inhibitor concentrations straddling the K_i value) of the inhibitor. To each of these solutions 50 μM CNP-fucoside was added to initiate hydrolysis. The K_i values were determined by analyzing the initial enzyme rates in the absence of inhibitor and comparing with the rate in the presence of increasing concentrations of inhibitor. The K_i value were calculated as the reciprocal of the gradient of each plot.

Antiproliferative assays

Cell culture: The breast-cancer cell line MDA-MB-231 was obtained from the American Type Cell Culture Collection (Rockville, MD, USA). Cell culture reagents were purchased from Lonza (Levallois-Perret, France). Cells were routinely grown in monolayers and maintained at 37°C in an atmosphere of 5% CO_2, in the Dulbecco modified eagle medium (DMEM) supplemented with 10% fetal bovine serum (FBS), 2 mM L-glutamine, 100 units mL^{-1} penicillin–streptomycin.

Proliferation assays: An aliquot of 2×10^3 cells were seeded in 96-well plates in DMEM, 10% FBS. The medium was replaced after 24 h, and the cells were treated for 48 h with 0, 25, and 50 μM of iminosugars. Cell numbers were determined by adding 3-(4,5-dimethylthiazol-2-yl)-5-(3-carboxymethoxyphenyl)-2-(4-sulfophenyl)-2*H*-tetrazolium (MTS) to the wells 2 h before spectrophotometric reading (absorbance at λ=490 nm). The results are expressed for each concentration of inhibitor for the control as mean value of 8 wells ± SD.

Acknowledgements

This work was supported by the University of Sciences and Technologies of Lille, the Association pour la Recherche sur le Cancer (Grant no. 7936 and 5023), the comité de l'Aisne de La Ligue contre le Cancer, and the Ministère de l'Enseignement Supérieur et de la Recherche (PhD studentship to A.H.). This work was also supported by the Biotechnology and Biological Sciences Research Council (BBSRC) through a PhD studentship to D.W.W. This work was carried out with the support of the Diamond Light Source. We thank Garib Murshudov for the generation of stereochemical target values and coordinate sets for ferrocenyl inhibitors **4a**,**c**.

[1] *Essentials of Glycobiology* (Eds.: A. Varki, R. Cummings, J. Esko, H. Freeze, P. Stanley, C. R. Bertozzi, G. Hart, M. E. Etzler), Cold Spring Harbor Laboratory Press, 2nd ed., **2009**.

[2] a) S. Hakomori, *Cancer Res.* **1996**, *56*, 5309–5318; b) S. Hakomori, *Proc. Natl. Acad. Sci. USA* **2002**, *99*, 10231–10233; c) Y. Y. Zhao, M. Takahashi, J. G. Gu, E. Miyoshi, A. Matsumoto, S. Kitazume, N. Tanigushi, *Cancer Sci.* **2008**, *99*, 1304–1310; d) A. Cazet, S. Julien, M. Bobowski, J. Burchell, P. Delannoy, *Breast Cancer Res.* **2010**, *12*, 204; e) D. L. Meany, D. W. Chan, *Clin. Proteomics* **2011**, *8*, 7.

[3] a) J. J. Listinsky, G. P. Siegal, C. M. Listinsky, *Am. J. Transl. Res.* **2011**, *3*, 292–322; b) D. J. Becker, J. B. Lowe, *Glycobiology* **2003**, *13*, 41R–53R.

[4] a) Q. Guo, B. Guo, Y. Wang, J. Wu, W. Jiang, S. Zhao, S. Qiao, Y. Wu, *Biochem. Biophys. Res. Commun.* **2012**, *417*, 311–317; b) K. Yuan, D. Kucik, R. K. Singh, C. M. Listinsky, J. J. Listinsky, G. P. Siegal, *Int. J. Oncology* **2008**, *32*, 797–807; c) J.-W. Wang, R. A. Ambros, P. W. Weber, T. G. Rosano, *Cancer Res.* **1995**, *55*, 3654–3658.

[5] T. Legigan, J. Clarhaut, I. Tranoy-Opalinski, A. Monvoisin, B. Renoux, M. Thomas, A. Le Pape, S. Lerondel, S. Papot, *Angew.*

Chem. **2012**, *124*, 11774–11778; *Angew. Chem. Int. Ed.* **2012**, *51*, 11606–11610.

[6] a) T. M. Gloster, G. J. Davies, *Org. Biomol. Chem.* **2010**, *8*, 305–320; b) *Iminosugars as Glycosidase Inhibitors: Nojirimycin and Beyond*, (Ed.: A. E. Stütz), Wiley-VCH, Weinheim, Germany, **1999**.

[7] a) *Iminosugars: From Synthesis to Therapeutic Applications*, (Ed.: P. Compain, O. R. Martin), Wiley, New York, **2007**; b) G. Horne, F. X. Wilson, J. Tinsley, D. H. Williams, R. Storer, *Drug Discovery Today* **2011**, *16*, 107–118; c) T. M. Wrodnigg, A. J. Steiner, B. J. Ueberbach, *Anticancer Agents Med. Chem.* **2008**, *8*, 77–85; d) B. G. Winchester, *Tetrahedron: Asymmetry* **2009**, *20*, 645–651; e) L. Zhang, F. Sun, Y. Li, X. Sun, X. Liu, Y. Huang, L.-H. Zhang, X.-S. Ye, J. Xiao, *ChemMedChem* **2007**, *2*, 1595–1597; f) H. Fiaux, D. A. Kuntz, D. Hoffman, R. C. Janzer, S. Gerber-Lemaire, D. R. Rose, L. Juillerat-Jeanneret, *Bioorg. Med. Chem.* **2008**, *16*, 7337–7346; g) H. Fiaux, F. Popowycz, S. Favre, C. Schütz, P. Vogel, S. Gerber-Lemaire, L. Juillerat-Jeanneret, *J. Med. Chem.* **2005**, *48*, 4237–4246; h) M. Padró, J. A. Castillo, L. Gomez, J. Joglar, P. Clapes, C. De Bolos, *Glycoconjugate J.* **2010**, *27*, 277–285; i) E. Moreno-Clavijo, A. T. Carmona, A. J. Moreno-Vargas, M. A. Rodriguez-Carvajal, I. Robina, *Bioorg. Med. Chem.* **2010**, *18*, 4648–4660.

[8] a) H.-J. Wu, C.-W. Ho, T.-P. Ko, S. D. Popat, C.-H. Lin, A. H.-J. Wang, *Angew. Chem.* **2010**, *122*, 347–350; *Angew. Chem. Int. Ed.* **2010**, *49*, 337–340; b) C.-H. Wu, C.-F. Chang, J. S.-Y. Chen, C.-H. Wong, C.-H. Lin, *Angew. Chem.* **2003**, *115*, 4809–4812; *Angew. Chem. Int. Ed.* **2003**, *42*, 4661–4664.

[9] a) E. Moreno-Clavijo, A. T. Carmona, A. J. Moreno-Vargas, L. Molina, I. Robina, *Curr. Org. Synth.* **2011**, *8*, 102–133; b) A. Ak, S. Prudent, D. LeNouën, A. Defoin, C. Tarnus, *Bioorg. Med. Chem. Lett.* **2010**, *20*, 7410–7413; c) M. S. M. Pearson, N. Floquet, C. Bello, P. Vogel, R. Plantier-Royon, J. Szymoniak, P. Bertus, J.-B. Behr, *Bioorg. Med. Chem.* **2009**, *17*, 8020–8026; d) A. J. Moreno-Vargas, A. T. Carmona, F. Mora, P. Vogel, I. Robina, *Chem. Commun.* **2005**, 4949–4951.

[10] a) E. Moreno-Clavijo, A. T. Carmona, Y. Vera-Ayoso, A. J. Moreno-Vargas, CC. Bello, P. Vogel, I. Robina, *Org. Biomol. Chem.* **2009**, *7*, 1192–1202; b) J.-B. Behr, *Tetrahedron Lett.* **2009**, *50*, 4498–4501; c) A. Kotland, F. Accadbled, K. Robeyns, J.-B. Behr, *J. Org. Chem.* **2011**, *76*, 4094–4098.

[11] a) A. Lammerts van Bueren, S. D. Popat, C.-H. Lin, G. J. Davies, *ChemBioChem* **2010**, *11*, 1971–1974; b) A. Lammerts van Bueren, A. Ardèvol, J. Fayers-Kerr, B. Luo, Y. Zhang, M. Sollogoub, Y. Blériot, C. Rovira, G. J. Davies, *J. Am. Chem. Soc.* **2010**, *132*, 1804–1806.

[12] A. Hottin, F. Dubar, A. Steenackers, P. Delannoy, C. Biot, J.-B. Behr, *Org. Biomol. Chem.* **2012**, *10*, 5592–5597.

[13] For examples of ferrocenylamine derivatives displaying anticancer activity, see: a) A. Mooney, R. Tiedt, T. Maghoub, N. O'Donovan, J. Crown, B. White, P. T. M. Kenny, *J. Med. Chem.* **2012**, *55*, 5455–5466; b) A. J. Salmon, M. L. Williams, Q. K. Wu, J. Morizzi, D. Gregg, S. A. Charman, D. Vullo, C. T. Supuran, S.-A. Poulsen, *J. Med. Chem.* **2012**, *55*, 5506–5517; c) H. Hagen, P. Marzenell, E. Jentzsch, F. Wenz, M. R. Veldwijk, A. Mokhir, *J. Med. Chem.* **2012**, *55*, 924–934.

[14] a) B. L. Stocker, E. M. Dangerfield, A. L. Win-Mason, G. W. Haslett, M. S. M. Timmer, *Eur. J. Org. Chem.* **2010**, 1615–1637; b) P. Compain, V. Chagnault, O. R. Martin, *Tetrahedron: Asymmetry* **2009**, *20*, 672–711.

[15] a) I. Gautier-Lefebvre, J.-B. Behr, G. Guillerm, M. Muzard, *Eur. J. Med. Chem.* **2005**, *40*, 1255–1261; b) A. Dondoni, P. P. Giovannini, D. Perrone, *J. Org. Chem.* **2002**, *67*, 7203–7214; c) A. Rives, Y. Génisson, V. Faugeroux, N. Saffon, M. Baltas, *Synthesis* **2009**, 3251–3258.

[16] A. M. Palmer, V. Jäger, *Eur. J. Org. Chem.* **2001**, 2547–2558.

[17] J.-B. Behr, M. S. M. Pearson, C. Bello, P. Vogel, R. Plantier-Royon, *Tetrahedron: Asymmetry* **2008**, *19*, 1829–1832.

[18] H. Fiaux, C. Schütz, P. Vogel, L. Juillerat-Jeanneret, S. Gerber-Lemaire, *Chimia* **2006**, *60*, 185–189.

[19] a) Y. L. Tan, P. Pigeon, S. Top, E. Labbé, O. Buriez, E. A. Hillard, A. Vessières, C. Amatore, W. K. Leong, G. Jaouen, *Dalton Trans.* **2012**, *41*, 7537–7549; b) D. Plazuk, S. Top, A. Vessières, M. A. Plamont, M. Huché, J. Zakrzewski, A. Makal, K. Woźniak, G. Jaouen, *Dalton Trans.* **2010**, *39*, 7444–7450.

[20] G. Sulzenbacher, C. Bignon, T. Nishimura, C. A. Tarling, S. G. Withers, B. Henrissat, Y. Bourne, *J. Biol. Chem.* **2003**, *279*, 13119–13128.

[21] D. A. Sela, D. Garrido, L. Lerno, S. A. Wu, K. M. Tan, H. J. Eom, A. Joachimiak, C. B. Lebrilla, D. A. Mills, *Appl. Environ. Microbiol.* **2012**, *78*, 795–803.

[22] a) A. Heine, E. A. Stura, J. T. Yli-Kauhaluoma, C. S. Gao, Q. L. Deng, B. R. Beno, K. N. Houk, K. D. Janda, I. A. Wilson, *Science* **1998**, *279*, 1934–1940; b) A. J. Salmon, M. L. Williams, A. Hofmann, S. A. Poulsen, *Chem. Commun.* **2012**, *48*, 2328–2330.

Received: March 15, 2013
Published online: ■■ ■■, 0000

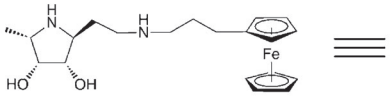

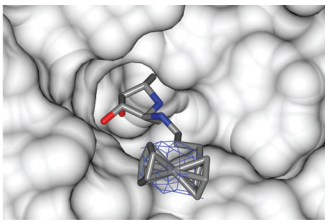

Transition-state-mimicking ^{3}E conformations (see picture) are evident from the three-dimensional structures of ferrocenyl iminosugar/fucosidase complexes. Novel pyrrolidine–ferrocene conjugates show strong anti-fucosidase and antiproliferative action, with up to 100% inhibition of proliferation of an MDA-MB-231 cancer-cell line at 50 μM.

Glycosidase Inhibitors

*A. Hottin, D. W. Wright, A. Steenackers, P. Delannoy, F. Dubar, C. Biot, G. J. Davies, J.-B. Behr** ..... ▮▮▮▮–▮▮▮▮

α-L-Fucosidase Inhibition by Pyrrolidine–Ferrocene Hybrids: Rationalization of Ligand-Binding Properties by Structural Studies